Opt Quant Electron (2016) 48:158
DOI 10.1007/s11082-016-0438-9

Polymer waveguide Bragg gratings made by laser patterning technique

David Mareš[1,2] · Vítězslav Jeřábek[1]

Received: 29 July 2015 / Accepted: 25 January 2016 / Published online: 2 February 2016

Abstract Planar waveguide gratings are very useful components for planar optical structures in which they function as wavelength optical filters, demultiplexers or sensors. The Bragg gratings formed on planar optical waveguides in multimode propagation regime show multiple reflections, which can lead to enlargement of the envelope of the dip transmission spectral characteristic. This paper reports on the design and measurement of the two types multimode planar optical waveguides with diffraction Bragg grating (PWBG) made on the core or cladding layer of the structure. In the first monostructural design, PWBG was made from an optical epoxy polymer SU-8. The second hybrid PWBG design was based on ion exchange $Ag^+ \leftrightarrow Na^+$ glass waveguide. A grating was made in polymethylmethacrylate cladding layer covering the waveguide. The third-order polymer PWBGs with grating constant $\Lambda_{q-3} = 1.35$ µm or $\Lambda_{q-3} = 1.2$ µm were prepared by new laser-thermal patterning technique based on Marangoni effect. Based on experimental and theoretical results, the topological parameters of the structures were optimized to obtain maximum diffraction efficiency of the polymer PWBG. The beam propagation method and the rigorous coupled-wave analysis were used in theoretical modelling, simulation and evaluation of designed PWBG dimension parameters. The Bragg wavelengths transmission dips were measured in NIR optical band at $\lambda = 1187$ nm or $\lambda = 1430$ nm, respectively. The spectral transmission attenuation dips were 10 and 15 dB corresponding to 90 and 97 % diffraction efficiency of polymer PWBGs. The advantage of multimode PWBGs and its applications are discussed.

Keywords Third-order Bragg grating · Multimode polymer waveguide · Epoxy polymer SU-8 · PMMA · Laser-thermal patterning

✉ Vítězslav Jeřábek
jerabek@fel.cvut.cz

1 Department of Microelectronics, Czech Technical University in Prague, Technická 2, 16627 Prague, Czech Republic

2 Research and Development, SQS Vláknová optika, a.s., 50901 Nová Paka, Czech Republic

1 Introduction

Planar optical waveguides with diffraction Bragg grating (PWBG) have been examined for planar spectral optical wavelength filtering, optical wavelength multiplexing and optical sensing in optical telecommunications and industrial applications. Over the last decade the PWBGs are subject of intense research. Optical polymers attract attention in mainly thanks to their unique characteristics, which are suitable for the implementation of PWBG integrated circuits. Due to the high light transmittance of some acrylates and epoxy polymers resulting in low optical insertion attenuation of around 0.03 db cm^{-1} (Ma et al. 2002), due to the environmental stability, cost efficiency and simple processing deposition steps, the polymers are well suited for increasingly more demanding requirements on the performance, degree of integration, cost efficiency and properties of modern PWBGs. Due to the large diversity of optical polymers and their properties, optimization of the structure characteristics for the selected application area can be achieved easily.

A number of devices using PWBGs, fabricated by different technology methods were presented in recent years. A tunable epoxy polymer SU-8 PWBG passband filter made by direct electron beam writing process was presented by Wong et al. (2003) and Zhu et al. (2005). Liu et al. (2014) presented PWBG wavelength tuning by temperature changes. The polymer grating-assisted coupler filter further improves the tuning efficiency and offers the 301-nm tuning ability (Zhang et al. 2014). PWBGs can also serve as add/drop multiplexers for WDM optical transmitters (Eldada et al. 1999; Katebi-Jahromi et al. 2012), fiber couplers (Wang et al. 2012) or mode converters presented by (Yang et al. 2014). In the majority of reported applications, Bragg grating (BG) works in a single mode regime. However, its use in few-mode and multimode regime, delivering wider band, was also presented by Mizunami et al. (2000). Beside its application in the optical telecommunication, PWBGs are also often used as optical sensors of temperature (Zhang and Tao 2013), strain or humidity (Rosenberg et al. 2012, 2014). Typical characteristics of the polymers, such as their large thermos-optic coefficient, higher Young's modulus or water absorption warrant the application of PWBGs as sensing devices.

In recent papers many methods of PWBG structures formation were proposed in different types of polymers. The common lithographic method is the contact UV photolithography, where the grating constant periodicity in the unit of micrometers is given by diffraction limit of the radiation exposure. Utilizing advanced X-ray photolithographic techniques (Reznikova et al. 2008), electron beam lithography EBL (Wong et al. 2003; and Zhu et al. 2005), focused ion beam writing FIB (Aubry et al. 2002) or nanoprinting (Ahn et al. 2005) it is possible to fabricate fine grating constant in hundreds of nanometers or less.

In this paper, we discuss the design, fabrication and measurement of two types multimode optical PWBGs, prepared by polymer PMMA-glass materials (hybrid composition) and the polymer SU-8 material (monostructure) for informatics and sensor application. The presented direct laser writing method (DLW), which uses the Marangoni phenomenon further simplifies the grating formation process (Luytakov et al. 2009, 2013; Kalachyova et al. 2014). The BMP and RCWA methods were used for theoretical modelling, optimization and evaluation of designed PWBG dimension parameters. The simulation results were compared to measurements of the optical spectral transmission characteristic of PWBGs.

2 Design and simulation of PWBG characteristics

Two technological and topological PWBG alternatives were proposed. The hybrid solution (design A) consist of a thin corrugated PMMA (polymethylmethacrylate) layer deposited on a sodium glass substrate with a diffused few-mode channel waveguide made by ion exchange $Ag^{+} \leftrightarrow Na^{+}$ (Barkman et al. 2013) Fig. 1a. The monostructure solution (design B), depicted in Fig. 1b, is formed by a corrugated ridge multi-mode waveguide made on SiO_2/Si or a borosilicate glass substrate.

The phase-matching Bragg condition can be written as $\vec{\beta}_d = \vec{\beta}_i + q\vec{K},\ q = 0, -1, -2, \ldots$, where $\vec{\beta}_d, \vec{\beta}_i$ are propagation vectors of diffracted and incident light, q is the order of the grating and $\vec{K}(|\vec{K}| = K = 2\pi/\Lambda)$ is the grating vector. For contradirectional propagated wave in 2D, where modules of propagated vectors are described as $\beta_i(|\vec{\beta_i}| = 2\pi N/\lambda_B), \beta_d = -\beta_i$, the condition for Bragg wavelength is then derived as $(\lambda_B = 2N\Lambda/q)$, where Λ is the period of the grating, N represents the effective index of refraction, λ_B is the Bragg wavelength and the q is the diffraction order. The calculated grating periods of PWBG for the first three orders Λ_q are summarized in Table 1.

The BeamPROP and GratingMOD software package from Synopsys Optical Solutions (SOS) were used for the design and optimization of PWBG structures. The simulations were focused on optimizing the thickness of the polymer grating layer T_{opt}, grating period for third order diffraction Λ_{q-3}, grating length L and grating modulation ratio *h/T* (modulation depth/thickness of layer). The aim of the optimization was the maximization of PWBGs diffraction efficiency η. The simulation of the fundamental transversal mode TE_0 distribution of design A indicates that a part of the guided light in the core of the ion channel penetrates the cladding layer and interacts with the grating. The refraction indices, optimal thickness of the cladding layer and the degree of the ion channel submersion had been optimized to allow for maximal interaction between the cladding layer and the submersed ion channel so that the radiation does not escape (couple out) from the diffuse waveguide. The optimal thickness of the cladding layer (design A) was found to be $T_{opt} = 500$ nm for the coupling coefficient $\kappa = 4.53\ \text{cm}^{-1}$ and the diffraction efficiency $\eta = 0.18$. The sufficient grating length $L = 5$ mm in the hybrid structure (design A) and $L = 1.3$ mm in monostructure (design B) were calculated to obtain diffraction efficiency $\eta > 95\ \%$. The calculation is shown in Fig. 2. The calculated results of the coupling coefficient κ, diffraction efficiency η for technologically achievable modulation depth $h < 800$ nm at Bragg wavelength $\lambda_B = 1200$ and 1450 nm are summarized in the Table 2.

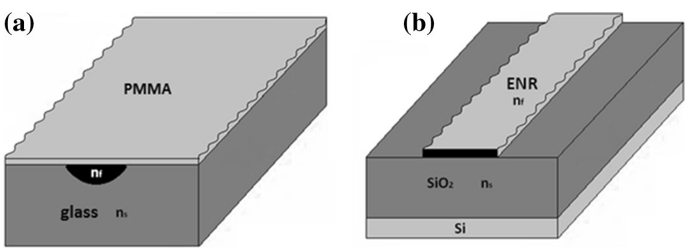

Fig. 1 Two topological alternatives of polymer PWBG: **a** PMMA cladding grating on the glass diffused waveguide (design A) **b** corrugated SU-8 core waveguide on SiO_2/Si substrate (design B)

Table 1 The calculated grating periods Λ_{q-1}, Λ_{q-2}, Λ_{q-3} of PWBG structures design A and design B for Bragg wavelength λ_B

	λ_B (nm)	N (−)	$\Lambda_{q=-1}$ (nm)	$\Lambda_{q=-2}$ (nm)	$\Lambda_{q=-3}$ (µm)
Design A	1200	1.4884	403	806	1.2
Design B	1450	1.5590	465	930	1.395

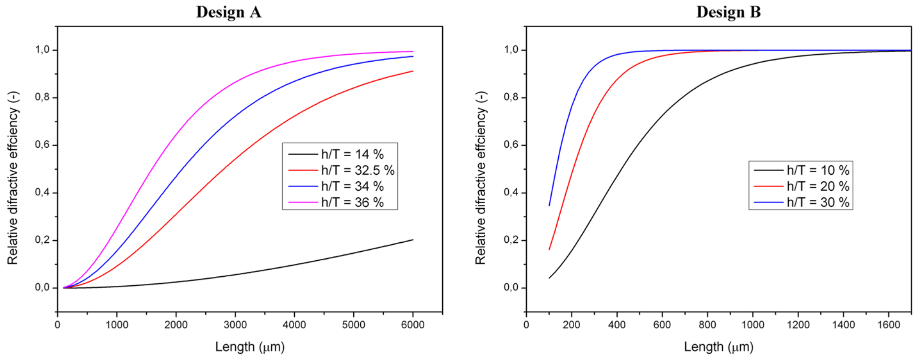

Fig. 2 Calculated diffraction efficiency η in dependence to the grating length L of Bragg reflection grating for different modulation depth/thickness layer ratio *h/T* as the parameter

Table 2 Calculated values of coupling coefficient κ and diffraction efficiency η for technologically achievable modulation ratio *h/T* of PWBG structures design A and B for wavelength $\lambda_B = 1200$ and 1450 nm

Design A Λ = 1.2 µm	T (nm)	h/T (%)	κ (cm)	η (−)	Design B Λ = 1.35 µm	T (nm)	h/T (%)	κ (cm)	η (−)
L = 1000 µm	400	32.5	4.09	0.15	L = 200 µm	2000	10	21.1	0.16
	500	36	4.53	0.18			20	42.8	0.48
	730	34	3.99	0.14			30	67.6	0.77
L = 5000 µm	500	36	4.53	0.97	L = 1300 µm	2000	10	21.1	0.95

3 Fabrication of designed PWBG

The mechanism of the laser patterning technique of the structure formation is based on the Marangoni effect polymer mass re-distribution (Malkin 2008) achieved by localized heat treatment. Due to the heat induced by absorbed laser radiation, the polymer is heated to the fluid temperature and starts melting. In order to increase the induced heat necessary to produce melting, the polymer had to be doped by an absorbing dye to enhance absorption at the wavelength of the used laser source. In the next step, the temperature gradient accompanied by surface tension gradient in the opposite direction is created by laser beam scanning. The resulting Marangoni phenomenon is causing the re-distribution of the polymer to the region with higher surface tension (lower temperature). The surface line of the future grating is formed. Finally, adding continuous mechanical movement of the sample in the parallel direction to scanning leads to the formation of the grating. The grating structure (the grating period and groove depth) is determined directly by the dopant concentration in the polymer, laser beam intensity and speed of the sample. The process is schematically depicted in Fig. 3.

The prepared polymer layer was subjected to a periodic thermal forming by a focused laser beam with an approximate diameter of 0.5 µm. The confocal laser scanning microscope Olympus Lext OLS 3100 operating at 405 nm wavelength, corresponding to the absorption band of doping dye was used as a laser source. The applied continuous wave laser power was set to 100 µW. The mechanical movement was provided by the piezoelectrically micro-controlled motor PMC-100 (Edmund Optics), which enabled the movement of the sample by a very small variable speed. The grating period was determined directly by the sample speed. The limitation of PMMA + Porphyrine grating profile layer was in the attainable value of grating period Λ_{q-3} for the wavelengths of 1000–1400 nm. The limitation of grating constant for the both polymers was set by minimum possible speed. The lower speed setting resulted in an irregular grating period. On the other hand, the maximum speed was limited by the threshold speed, at which the polymer surface is efficiently melted so as to create a grating with sufficient groove depth. In the case of SU-8 polymer, the regular gratings were created for the radiation wavelengths of 1300–1600 nm for the third order diffraction gratings. The fabrication procedure of polymer PWBG design A is described by the Fig. 4a–g.

The hybrid PWBG was formed on the PMMA layer deposited on the glass waveguide. The BG diffracted the evanescent waves of the guided modes propagated in the waveguide. The evanescent waves penetrated through a very thin cladding layer and interacted with the BG. To enhance the coupling of the evanescent waves to the BG, only one step of the ion

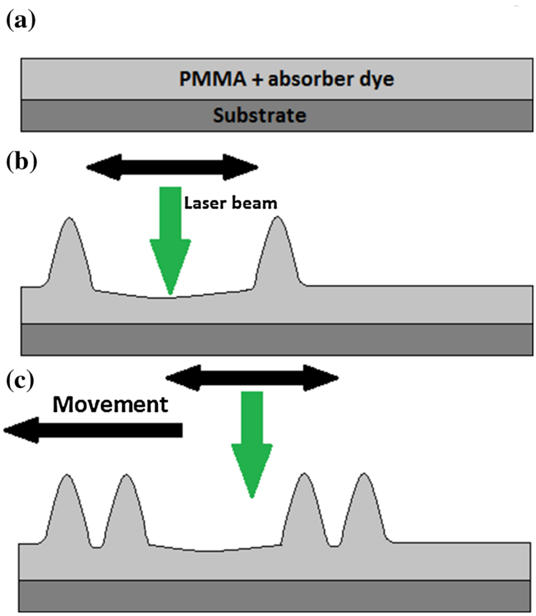

Fig. 3 Principle of PMMA laser pattering doped by absorbing dye: **a** intact featureless polymer surface, **b** surface distortion after the laser scanning on motionless sample surface and **c** lattice pattern is step-by-step induced by laser scanning by simultaneous mechanical movement of the sample

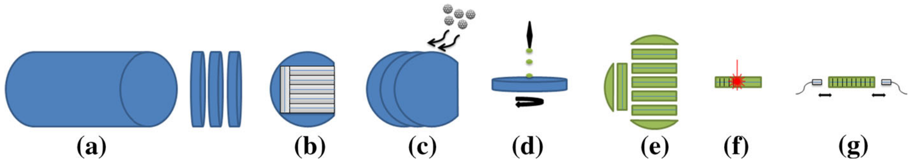

Fig. 4 The fabrication procedure of hybrid polymer PWBG—design A: **a** wafer cutting and polishing, **b** photolithography, **c** ion exchange, **d** polymer spin-coating, **e** chip cutting and polishing, **f** grating formation, **g** fiber-chip coupling

exchange $Ag^{+} \leftrightarrow Na^{+}$ to the glass was completed. Therefore, the channel was not buried but laid close to the surface of the glass substrate. The diffused channel waveguide had the refractive index of glass substrate of 1.492, refractive index difference of 0.003 and the channel diameter of 4 μm. The polymer PMMA with the dye additive Porphyrine has the refractive index of 1.485, when the pure PMMA exhibits refractive index of 1.477 at the wavelength of 1200 nm. The refractive index of the polymer mixture was set slightly below the refractive index of the waveguide glass core of 1.495. This small difference increased the penetration depth of the evanescent field and, at the same time, ensured a low loss of the guided modes in the core of the waveguide. The polymer mixture was then deposited on the cleaned and polished waveguide surface by spin-coating. In the next step, the PMMA grating layer was shaped by the confocal 405-nm laser patterning technique. Finally, the input and output standard single-mode fibers 9/125 μm placed in v-groove were butt-coupled to the polished facet of the waveguide grating and fixed by the UV curing glue with the matched refraction index. The photo and the AFM surface image of the prepared hybrid PWBG structure design A is shown in Fig. 5. The suppliers of the PMMA, SU-8 polymer and absorbing dye Porfyphirine were Goodfellow Inc., MicroChem and Frontier Scientific Inc., respectively.

The polymer monostructure PWBG (design B) was made by the UV photolithographic process with the negative photoresist SU-8. In the first step of PWBG fabrication, the epoxy polymer SU-8 layer was deposited on the substrate SiO_2/Si by spin-coating. The refractive indices of the SU-8 layer and SiO_2 substrate were n = 1.568 and n = 1.444 at $\lambda = 1450$ nm, respectively. A bulk dye doping of SU-8 polymer was not used, because Porphyrine dye prevents the UV cross-linking of the polymer. To overcome this issue, an additional Porphyrine dye layer was superimposed on the polymer SU-8 layer by vapor deposition. In the next step the patterning of grating through the dye layer was done by

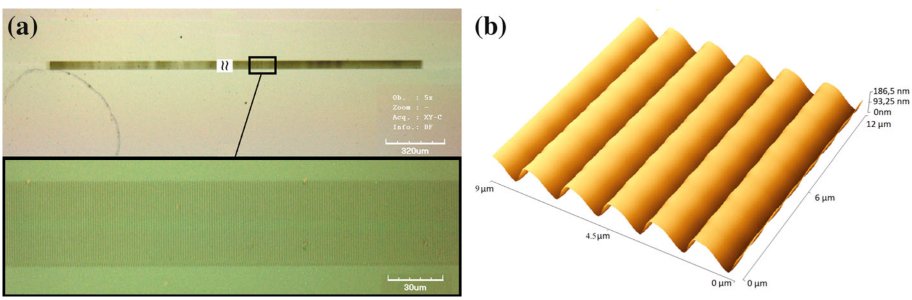

Fig. 5 **a** The fabricated PWBG with an ion exchange channel waveguide (design A). The grating period is $\Lambda_{q-3} = 1.2$ μm and length $L = 5$ mm. **b** AFM surface image of the PWBG

scanning of confocal laser microscope by wavelength of 405 nm. After the grating formation was completed, the dye layer was removed. The ridge waveguides were then prepared by the UV photolithographic procedure through a perpendicularly adjusted chrome mask on the formed grating structures. The procedure is shown in Fig. 6a–f.

The image of the fabricated structure is shown in Fig. 7a. In order to minimize the excessive loss caused by in/out light coupling, the focused ion beam etching was used to polish the end facets of the waveguides. In order to prepare the monostructure PWBG design B, the FIB-SEM enhancing method was used, which allowed simultaneous ion beam etching FIB followed by SEM image, see Fig. 7b. The roughness of the end facets was ascertained from SEM images of the end facets. The images were done with the resolution of 5 nm per pixel. Based on the resulting images it was concluded that the roughness of the end facets was below RMS = 30 nm.

4 Measurement of fabricated samples, results and discussion

The fabricated samples were measured with the use of the system/setup for the measurement of the optical spectral transmission power. The halogen lamp was used as the broadband source emitting in the wavelength range of 360–2400 nm. While using the optical fiber or focusing microscope objectives, this source was optically coupled with the input facet of PWBG. The output facet was connected to the optical spectral analyzer Yokogawa AQ6370C with a bandwidth of 600–1700 nm. The samples of the PWBG hybrid design were equipped with SM optical fibers with FC connectors. The PWBG designs B samples were coupled by microscope objectives to the facet of SU-8 polymer optical waveguides and adjusted by a ten-axis micromanipulator. The optical spectral transmission characteristics of the fabricated samples are shown in Fig. 8. The significant dips for design A at $\lambda = 1187$ nm and for design B at $\lambda = 1430$ nm were observed. The spectral transmission attenuations were 10 and 15 dB in the dip. The attenuation is equal to 90 and 97 % diffraction efficiency for PWBG design A and design B respectively. The measured wavelengths value were close to the designed Bragg wavelengths ($\lambda = 1200$ nm and $\lambda = 1450$ nm). We attribute the differences between the targeted and measured wavelengths to a mismatch between the value of the effective refractive index used in our calculations and simulations and the actual value. A number of dips located around the central wavelength from the multimode waveguide regime were observed in the measured spectral characteristics of PWBG. The typical measured insertion loss of PWBG (design A) was $IL_A = 3.2$ dB at the wavelength of 1550 nm, the loss of design B was $IL_B = 5.1$ dB at the wavelength of 1310 nm and $IL_B = 7.3$ dB at the wavelength of 1550 nm.

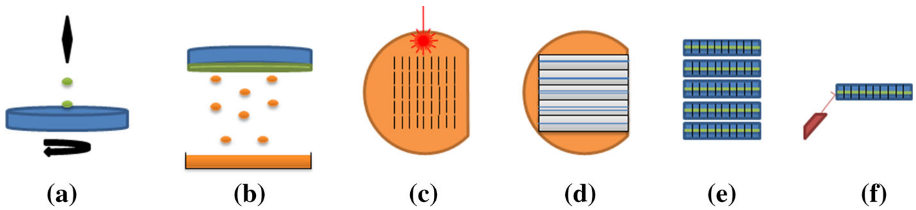

Fig. 6 The fabrication procedure of polymer PWBG design B: **a** polymer spin-coating, **b** dye casting, **c** laser patterning, **d** photolithography, **e** chip cutting, **f** FIB facet etching

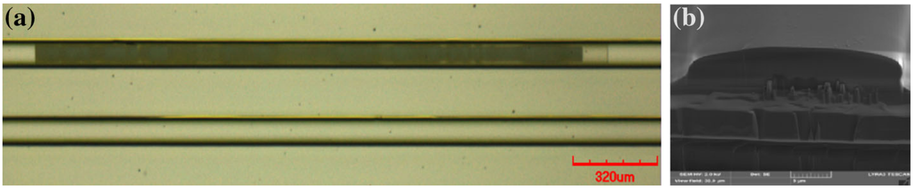

Fig. 7 **a** The fabricated PWBG on ridge waveguide with grating period $\Lambda_{q-3} = 1.35$ µm and length $L = 1.3$ mm (design B). *Upper part* shows the PWBG fabricated on ridge waveguide, the *lower part* shows unmodified ridge waveguide for dimensions of the waveguide core 5 µm × 2 µm. **b** SEM image of the SU8 facet polished by FIB method

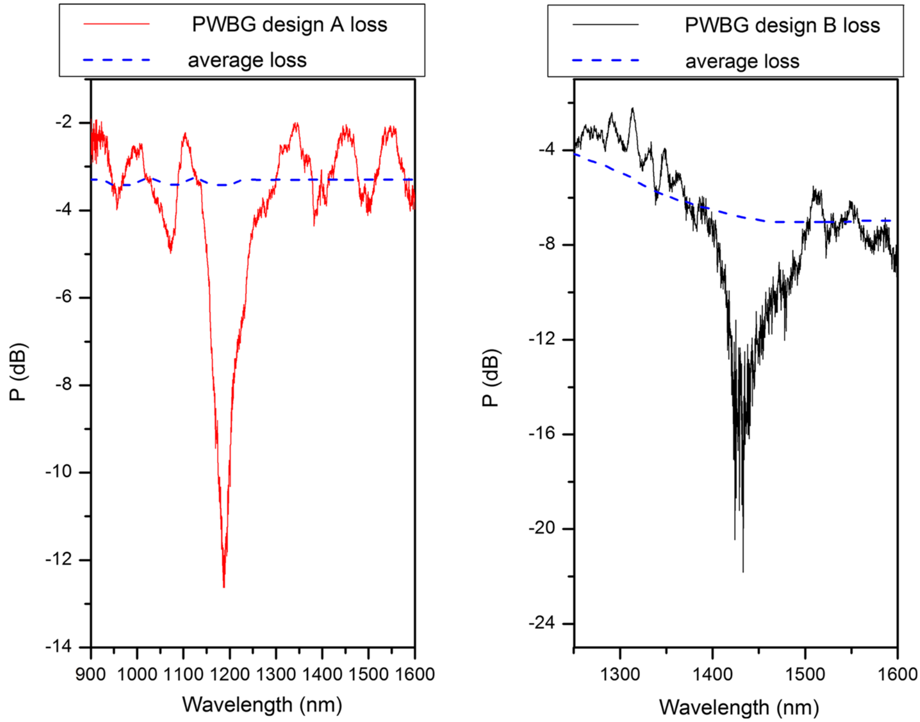

Fig. 8 Optical spectral transmission characteristic of fabricated PWBG samples design A and B

The optical loss of the polymer waveguide itself was measured and specified using the cut-back method (Christian and Passauer 1990). The optical waveguide loss was calculated by (1)

$$\alpha\left(dB \cdot \mathrm{cm}^{-1}\right) = \frac{10 \cdot \log \frac{P_1(W)}{P_2(W)}}{l_1 - l_2\,(\mathrm{cm})} \tag{1}$$

where P_1 is the output optical power measured over the whole length of the waveguide l_1, P_2 is the output optical power obtained after breaking the waveguide, l_2 is the length of the broken part of the optical waveguide. The measurement was performed at the wavelength of 1310 and 1550 nm. The output light from the waveguides was measured by the optical power meter Thorlabs PM200 and the S155C probe. The typical optical waveguide loss of design B samples was measured by the cut-back method to be $\alpha = 1.5$ dB/cm at wavelength of 1310 nm and $\alpha = 2.3$ dB/cm wavelength of 1550 nm. The coupling losses of 1-cm long of the design B sample were calculated by the subtraction insertion and waveguide losses as $IL_B = 3.6$ dB at wavelength of 1310 nm and $IL_B = 5$ dB at wavelength of 1550 nm.

5 Conclusion

The planar optical multi-mode waveguides with PWBG have been investigated. Two types of the polymer PWBGs were designed, fabricated and measured. In the first monostructural design, PWBG was made from an optical epoxy polymer SU-8. The second hybrid PWBG design was based on ion exchange $Ag^+ \leftrightarrow Na^+$ glass waveguide. A grating was made in PMMA cladding layer covering the waveguide. The BGs were made by new method of the laser-thermal patterning technique based on Marangoni effect. This technique produced smooth and sinusoidal profiled surface gratings without any defects. The structures were made by a new technological process. The number of the needed process steps is lower and the formation speed of the polymer grating is higher in comparison to other advanced methods. The technology procedure does not need any specialized equipment and lithography. The DLW produces smooth, almost sinusoidal, surface shaping without any defects. The presented method contributes to an easy production of polymer PWBGs. Additionally, using additives of selected monomers enables to control the final refractive index by copolymerization degree of base polymer. Based on the experimental and theoretical results, the topological parameters of the structures were optimized to obtain maximum diffraction efficiency of the polymer PWBG. The BMP and RCWA were used for theoretical modelling, simulation and evaluation of designed PWBG dimension parameters. The third-order polymer PWBGs with the grating constant $\Lambda_{q-3} = 1.35$ µm or $\Lambda_{q-3} = 1.2$ µm was fabricated. The fabricated polymer PWBGs exhibit third order diffraction documented by measurement of the optical spectral transmission characteristics. The spectral position of the Bragg dips for design A at $\lambda = 1187$ nm and for design B at $\lambda = 1430$ nm correspond to our calculations. The measured optical spectral transmission attenuations in dips were 10 dB and 15 dB, which is equal to the diffraction efficiency of 90 and 97 %. The measured insertion losses of PWBG were $IL_A = 3.2$ dB and $IL_B = 5.1$ dB at wavelength of 1310 nm. The higher insertion losses of the design B at different wavelengths was caused by the wavelength dependence coupling of the microscope objectives. The typical optical waveguide loss was measured by cut-back method to be $\alpha = 1.5$ dB/cm at wavelength of 1310 nm and $\alpha = 2.3$ dB/cm at wavelength of 1550 nm. The advantage of these designed PWBGs is in its few/multimode design, which enables a relatively broadband filtration (FHWM up to 20 nm) and delivers high diffraction efficiency. PWBG can be used for planar spectral optical broadband filtering, optical two band wavelength multiplexing and optical sensing in the optical communication and sensors. The gratings can be combined for instance with Y power splitter as the integrated optical wavelength broadband demultiplexer.

Acknowledgments The research was done in a productive collaboration with ICT Prague, Department of Solid State Engineering, Institute of Chemical Technology and SQS Vláknová optika a.s. company. This work was supported in part by the Student Grant Competition of the Czech Technical University in Prague under the Grant Number of SGS16/057/OHK3/2T/16.

References

Ahn, S.W., Lee, K.D., Kim, D.H., Lee, S.S.: Polymeric wavelength filter based on a Bragg grating using nanoimprint technique. IEEE Photon. Technol. Lett. **17**, 2122–2124 (2005)

Aubry, C., Trigaud, T., Moliton, J.P., Chiron, D.: Polymer gratings achieved by focused ion beam. Synt. Met. **127**, 307–311 (2002)

Barkman, O., Jeřábek V., Prajzler, V.: Optical splitters based on self-imaging effect in multi-mode waveguide made by ion exchange in glass. Radioengineering **22**, 352–356 (2013)

Christian, N.L., Passauer, L.K.: Fiber Optics Component, Design, Fabrication, Testing Operation, Reliability and Maintainability. William Andrew Publishing, Norwich (1990)

Eldada, L., Blomquist, R., Maxfield, M., Pant, D., Boudoughian, G., Poga, C., Norwood, R.: Thermooptic planar polymer Bragg grating OADMs with broad tuning range. IEEE Photon. Technol. Lett. **11**, 448–450 (1999)

Kalachyova, Y., Lyutakov, O., Slepicka, P., Elashnikov, R., Svorcik, V.: Preparation of periodic surface structures on doped poly(methyl metacrylate) films by irradiation with KrF excimer laser. Nanoscale Res. Lett. **9**, 591 (2014)

Katebi-Jahromi, A., Karimi-Alavijeh, H., Jalilpiran, S., Arianfard, H., Gharavi, A.: Integrated 1 × 2 polymeric add/drop multiplexer. J. Lightwave Technol. **30**, 700–703 (2012)

Liu, A., Zhang, Z., de Felipe, D., Keil, N., Grote, N.: Power-efficient thermo-optic tunable filters based on polymeric waveguide Bragg gratings. IEEE Photon. Technol. Lett. **26**, 313–315 (2014)

Lyutakov, O., Hüttel, I., Siegel, J., Švorčík, V.: Regular surface grating on doped polymer induced by laser scanning. Appl. Phys. Lett. **95**, 173103 (2009)

Lyutakov, O., Tuma, J., Huttel, I., Prajzler, V., Siegel, J., Svorcik, V.: Polymer surface pattering by laser scanning. Appl. Phys. B **110**, 539–549 (2013)

Ma, H., Jen, A.K.Y., Dalton, L.R.: Polymer based optical waveguides: materials, processing and devices. Adv. Mater. **14**, 1339–1365 (2002)

Malkin, A.Y.: Surface instabilities. Colloid J. **70**, 673–689 (2008)

Mizunami, T., Djambova, T.V., Niiho, T., Gupta, S.: Bragg gratings in multimode and few-mode optical fibers. J. Lightwave Technol. **18**(2), 230 (2000)

Reznikova, E., Mohr, J., Boerner, M., Nazmov, V., Jakobs, P.J.: Soft X-ray lithography of high aspect ratio SU8 submicron structures. Microsys. Technol. **14**, 1683–1688 (2008)

Rosenberger, M., Koller, G., Belle, S., Schmauss, B., Hellmann, R.: Planar Bragg grating in bulk polymethylmethacrylate. Opt. Express **20**, 27288–27296 (2012)

Rosenberger, M., Hessler, S., Belle, S., Schmauss, B., Hellmann, R.: Compressive and tensile strain sensing using a polymer planar Bragg grating. Opt. Express **22**, 5483–5490 (2014)

Wang, L., Li, Y., Porcel, M.G., Vermeulen, D., Han, X., Wang, J., Jian, X., Baets, R., Zhao, M., Morthier, G.: A polymer-based surface grating coupler with an embedded Si_3N_4 layer. J. Appl. Phys. **111**, 114507 (2012)

Wong, W.H., Pun, E.Y.B., Chan, K.S.: Electron beam direct-write tunable polymeric waveguide grating filter. IEEE Photon. Technol. Lett. **15**, 1731–1733 (2003)

Yang, Y., Chen, K., Jin, W., Chiang, K.S.: Mode converter with polymer long-period waveguide grating. In: Asia Communications and Photonics Conference Optical Society of America, AW4C.4 (2014)

Zhang, Z.F., Tao, X.M.: Intrinsic temperature sensitivity of fiber Bragg gratings in PMMA-based optical fibers. IEEE Photon. Technol. Lett. **25**, 310–312 (2013)

Zhang, Z., Maese-Novo, A., Schwartz, E., Zawadzki, C., Keil, N.: 301-nm wavelength tunable differentially driven all-polymer optical filter. Opt. Lett. **39**, 5170–5172 (2014)

Zhu, L., Huang, Y., Green, W., Yariv, A.: Tunable transmission filters based on corrugated sidewall Bragg gratings in polymer waveguides. In: Conference on Lasers and Electro-Optics. Optical Society of America, (2005)